

## Catalyzed $\text{Na}_2\text{LiAlH}_6$ for hydrogen storage

X.Z. Ma<sup>a,\*</sup>, E. Martinez-Franco<sup>a,b,1</sup>, M. Dornheim<sup>a</sup>, T. Klassen<sup>a</sup>, R. Bormann<sup>a</sup>

<sup>a</sup> Institute for Materials Research, GKSS Research Center, DE-21502 Geesthacht, Germany

<sup>b</sup> ESIQIE-ZPN Metallurgical Department, IPN avenue s/n, Lindarista 07300, Mexico

Received 2 July 2004; received in revised form 15 October 2004; accepted 21 October 2004

Available online 18 July 2005

### Abstract

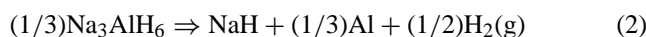
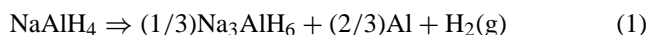
In the present study, the complex alanate  $\text{Na}_2\text{LiAlH}_6$  is synthesized by high-energy milling of powder blends containing NaH and  $\text{LiAlH}_4$ . The related thermodynamics are determined. In addition, a comprehensive study was performed to investigate the influence of different oxide and halide catalysts on the kinetics of hydrogen absorption and desorption, as well as their general drawback to decrease storage capacity.

© 2005 Elsevier B.V. All rights reserved.

**Keywords:** Alanate; High-energy ball milling; Catalyst; Hydrogen storage

### 1. Introduction

Hydrogen is regarded as the ideal means of energy storage for transportation and conversion of energy in a comprehensive clean-energy concept. One of the main problems to be solved is the storage of hydrogen. Metal hydrides offer a safe alternative for hydrogen storage and, in addition, have a high volumetric energy density. Among the hydrides, alanates are promising due to their high capacity by weight. However, alanates had not been considered as hydrogen storage materials until Bogdanovic et al. showed that rehydrogenation is possible in sodium alanate ( $\text{NaAlH}_4$ ) using titanium based materials as catalysts [1–3]. Thus, alanates have a technical potential for reversible hydrogen storage. Pure alanates liberate hydrogen through the following paths (taking  $\text{NaAlH}_4$  as an example):



Only Eqs. (1) and (2) are technically considered useful for reversible hydrogen storage, because temperature for the decomposition of NaH is rather high. Therefore, the technically accessible capacities for  $\text{NaAlH}_4$  or  $\text{LiAlH}_4$  are 5.6 or 7.9 wt.%, respectively. The equilibrium pressure for Eq. (2) is below 25 bar at a temperature lower than 200 °C [2]. For Eq. (1), the plateau pressure at 200 °C is about 150 bar, at 160 °C about 85 bar [2].

Regarding kinetics, the second reaction step is significantly slower than the first, and thus any improvements are more challenging. In this study, we therefore focus on Eq. (2). Furthermore, if Li may partially replace for Na, hydrogen storage capacities could be increased. Chemical synthesis of  $\text{Na}_2\text{LiAlH}_6$  and thermodynamic data at 211 °C for the material doped with Ti-based catalyst were reported in Ref. [1]. Hout et al. prepared the same material by ball-milling technique recently [4]. In a former paper [5] we presented our results on the synthesis of  $\text{Na}_x\text{Li}_{3-x}\text{AlH}_6$  by ball milling of different hydrides. Besides  $\text{Na}_3\text{AlH}_6$  and  $\text{Li}_3\text{AlH}_6$  the phase  $\text{Na}_2\text{LiAlH}_6$  has been successfully obtained by this method. However, detailed studies of the thermodynamic properties of  $\text{Na}_2\text{LiAlH}_6$  are still lacking. Furthermore, it has been shown that oxides and halides lead to a significant improvement in kinetics for  $\text{MgH}_2$  and  $\text{NaAlH}_4$ .

In the present study, the thermodynamic and kinetic properties of  $\text{Na}_2\text{LiAlH}_6$  modified by different halide and ox-

\* Corresponding author. Tel.: +49 4152 872554; fax: +49 4152 872636.

E-mail address: xuezhu.ma@gkss.de (X.Z. Ma).

<sup>1</sup> Current address: CIITec-IPN, Cerrada de Cecati s/n, Santa Catarina 02250, Mexico.

ide catalysts are investigated with the aim to achieve the best compromise between hydrogen capacity and sorption kinetics.

## 2. Experimental

The milling experiments were performed in a Fritsch P5 planetary ball mill at a speed of 230 rpm, using hardened Cr-steel milling tools and an initial ball-to-powder weight ratio of 400 g:40 g. The starting materials were  $\text{LiAlH}_4$  (97%, ABCR Karlsruhe, Germany), and  $\text{NaH}$  (95%, Aldrich Chemical Co. Inc.). Catalysts used in this study were purchased from Sigma–Aldrich Company with a purity of 99.5% or higher. Raw materials were weighed in the desired overall ratio, then blended and milled for typically 100 h. Specimens were taken after different milling times. All handling of the powders (including weighing, loading, milling) were performed inside a glove box under continuously purified argon atmosphere (oxygen, and water content each below 10 ppm). For determination of the sorption properties (including kinetic measurements and pressure–concentration–isotherm (PCT) measurements), specimen holders were sealed inside the glove box and attached to a hydrogen titration apparatus (Model: C2-3000, HERA, Canada), which was especially designed for fast data acquisition. This system covers the temperature range from room temperature to 400 °C at hydrogen pressures up to 200 bar. For measurements of the desorption kinetics, the chamber was evacuated to  $10^{-3}$  mbar. The mass of each specimen could vary randomly in the range of 100 mg to a few grams by choosing different size sample holders.

X-ray diffraction (XRD) samples were also prepared in the glove box. To avoid exposure to air, the samples were covered with plastic foil, which had a negligible and easily deductible contribution to the diffraction patterns. The powders at different experimental stages were characterized by X-ray diffractometry (Bruker D8 Advance) using  $\text{Cu K}\alpha$  radiation ( $\lambda = 1.5406 \text{ \AA}$ ). The patterns were scanned by steps of  $0.05^\circ$  ( $2\theta$ ) with a counting time of 3 s.

## 3. Results and discussion

PCT data were recorded out to study the thermodynamic properties of  $\text{Na}_2\text{LiAlH}_6$ . Respective results are listed in Table 1.  $\text{Na}_2\text{LiAlH}_6$  is a typical medium temperature hydrogen storage material with plateau pressures below 25 bar in the temperature range of 180–230 °C. The calculated reaction enthalpy according Van't Hoff diagram is determined as  $-23 \text{ kJ/mol H}_2$ , details and discussion will be presented in a forthcoming paper [6].

Fig. 1 shows the phase evolution upon milling and after absorption for a  $\text{LiAlH}_4/2\text{NaH}$  powder blend containing 2 mol%  $\text{CeO}_2$ . After 30 min milling time, peaks relating to  $\text{Na}_2\text{LiAlH}_6$  are observed, documenting the phase reaction between the two hydrides  $\text{LiAlH}_4$  and  $\text{NaH}$ . After 2 h milling

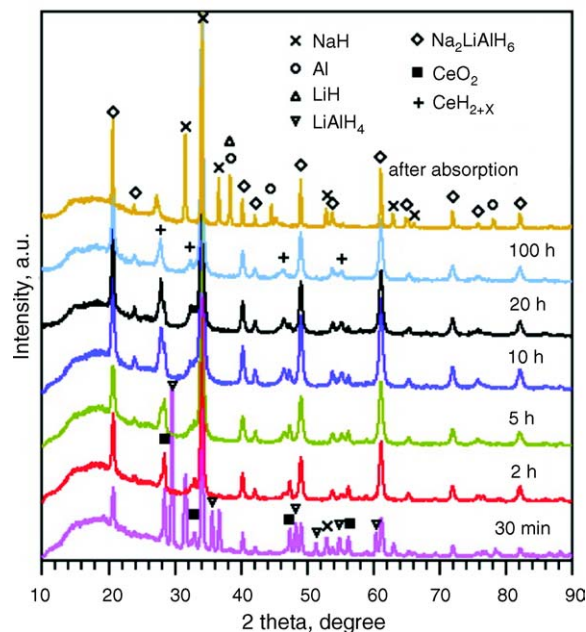


Fig. 1. XRD patterns for a  $\text{LiAlH}_4/2\text{NaH}$  powder blend containing 2 mol%  $\text{CeO}_2$  after different milling times and after absorption.

time, the diffraction peaks for  $\text{LiAlH}_4$  have disappeared completely, and  $\text{Na}_2\text{LiAlH}_6$  becomes the dominating phase. In addition, the main peaks for the catalyst  $\text{CeO}_2$  can also be detected. In the XRD pattern after absorption, residual  $\text{NaH}$ ,  $\text{Al}$  and  $\text{LiH}$  can be observed, indicating that the reaction is not fully completed. The four strongest diffraction peaks of  $\text{CeO}_2$  at  $28.55^\circ$ ,  $33.08^\circ$ ,  $47.49^\circ$  and  $56.33^\circ$  (diffraction angle  $2\theta$ ) are marked by black squares in Fig. 1. With increasing milling time the intensity for  $\text{CeO}_2$  decreases and a new peak belonging to the phase  $\text{CeH}_{2+x}$  are detected (Fig. 2). At a milling time of 100 h, the  $\text{CeO}_2$  peaks have completely vanished. After absorption, the peaks of  $\text{CeH}_{2+x}$  are apparently shifted to lower angles, i.e. the main peaks now are observed at  $27.25^\circ$  and  $45.39^\circ$ , respectively. This would correspond to a lattice expansion of about 2.2%, which indicates a change in hydrogen concentration in the Ce. However, it is yet unclear, whether the formation of  $\text{CeH}_{2+x}$  plays any promoting role for the hydrogen reaction.

As another example, XRD patterns after different milling time and after absorption for a  $\text{LiAlH}_4/2\text{NaH}$  powder blend containing 2 mol% of  $\text{TiCl}_3$  are shown in Fig. 3. There is an obvious difference in phase reaction between  $\text{Na}_2\text{LiAlH}_6$  containing  $\text{TiCl}_3$  or  $\text{CeO}_2$ . While cerium contained phases

Table 1

Absorption and desorption pressure plateaus for  $\text{Na}_2\text{LiAlH}_6$ , as obtained from PCT diagrams. The pressure gauge does not allow for accurate determination of pressures lower than 1 bar

$T$ (°C)	$P_{\text{abs}}$ (atm)	$P_{\text{des}}$ (atm)
180	9	$\ll 1$
200	13	$< 1$
220	20	3.95
230	21	9.87

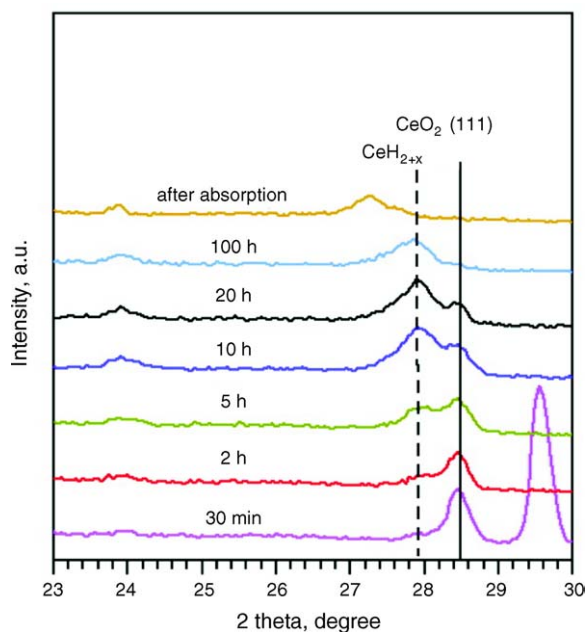


Fig. 2. A close-up of Fig. 1 showing the decrease of peak intensity for  $\text{CeO}_2$  and the formation of  $\text{CeH}_{2+x}$  upon milling.

are always observed in the case of  $\text{CeO}_2$ ,  $\text{TiCl}_3$  cannot be detected anymore after 5 h milling. Instead, a reaction between the hydride and  $\text{TiCl}_3$  is observed as also found in previous investigations [7,8] on  $\text{NaAlH}_4$ . Thus,  $\text{NaCl}$  is formed after short time milling, which most probably does not take part anymore in the hydrogen reaction, but reduces the overall capacity.

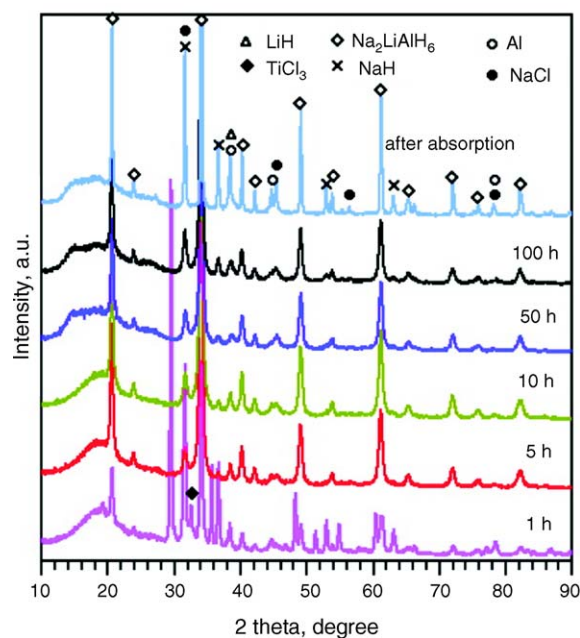


Fig. 3. XRD patterns for a  $\text{LiAlH}_4/2\text{NaH}$  powder blend containing 2 mol%  $\text{TiCl}_3$  after different milling time and after absorption. The unmarked peaks after 1 h milling time belong to the starting material  $\text{LiAlH}_4$ .

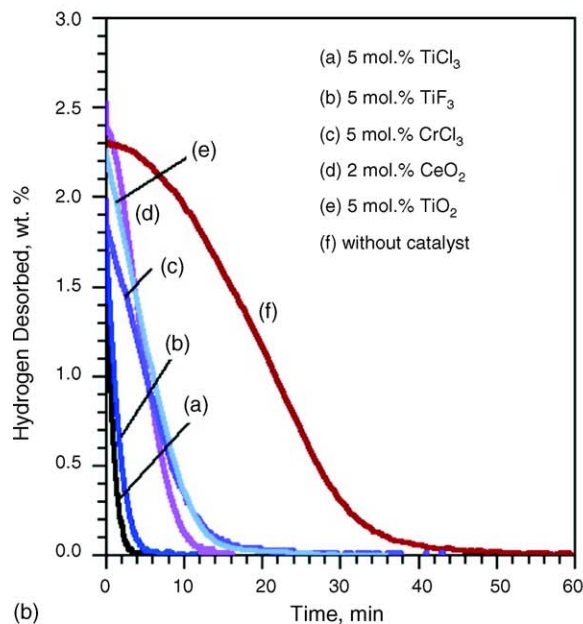
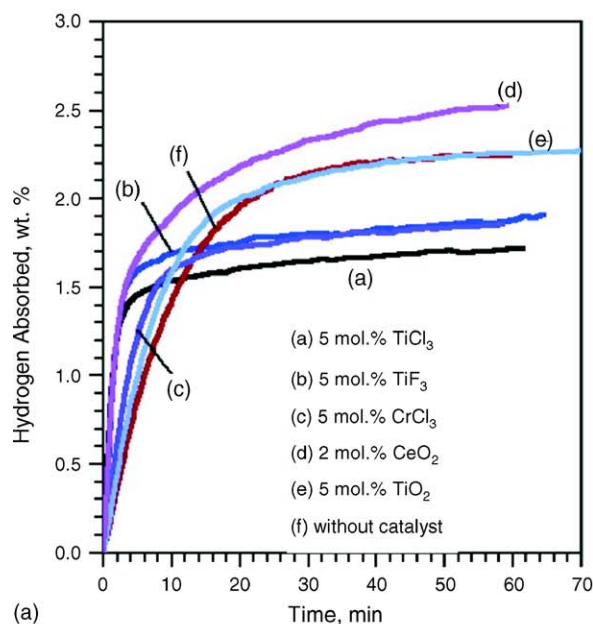


Fig. 4. Absorption and desorption kinetics for  $\text{Na}_2\text{LiAlH}_6$  with different catalysts after 100 h of milling. Absorption at  $230^\circ\text{C}$  under 43 bar, desorption at  $230^\circ\text{C}$  under a pressure of 0.55 bar.

Sorption kinetics achieved by some typical catalysts is shown in Fig. 4. Catalytic effects on absorption are not as pronounced as on desorption.  $\text{TiCl}_3$  shows the strongest effects on the kinetics of the sorption reactions, followed by  $\text{TiF}_3$ ,  $\text{CeO}_2$ ,  $\text{TiO}_2$  and  $\text{CrCl}_3$ . Reversible capacities for  $\text{TiCl}_3$ ,  $\text{TiF}_3$  and  $\text{CrCl}_3$  modified  $\text{Na}_2\text{LiAlH}_6$  are below 2.0 wt.% due to  $\text{NaCl}$  formation and incomplete absorption reactions. Even for  $\text{TiCl}_3$  contents as low as 0.5 mol%, the reversible hydrogen storage capacity is less than 2.0 wt.%. The highest capacity is achieved in  $\text{Na}_2\text{LiAlH}_6$  with 2 mol%  $\text{CeO}_2$ . In this material 2.6 wt.% hydrogen can be absorbed within 1 h and desorbed within 12 min at  $230^\circ\text{C}$ .  $\text{Na}_2\text{LiAlH}_6$  with 5 mol%

Table 2  
Absorption and desorption rates for Na<sub>2</sub>LiAlH<sub>6</sub> with different catalysts

Catalyst and content	Absorption rate (wt.%/min)	Desorption rate (wt.%/min)
5 mol% TiFe <sub>3</sub>	0.57	0.57
5 mol% TiCl <sub>3</sub>	0.51	0.60
2 mol% CeO <sub>2</sub>	0.48	0.31
5 mol% ZrCl <sub>4</sub>	0.46	0.27
5 mol% TiBr <sub>4</sub>	0.35	0.37
5 mol% CrCl <sub>3</sub>	0.23	0.15
2 mol% AlCl <sub>3</sub>	0.19	0.09
5 mol% TiO <sub>2</sub>	0.18	0.23
2 mol% Y <sub>2</sub> O <sub>3</sub>	0.17	0.19
5 mol% MnCl <sub>2</sub>	0.16	0.11
Without catalyst	0.15	0.08
5 mol% HfCl <sub>4</sub>	–	0.19

Absorption under 230 °C/43 bar, desorption under 230 °C/0.55 bar.

TiO<sub>2</sub> and Na<sub>2</sub>LiAlH<sub>6</sub> without catalyst reach a capacity of about 2.3 wt. %.

Other catalysts were also applied in the present study, such as AlCl<sub>3</sub>, HfCl<sub>4</sub>, ZrCl<sub>4</sub>, MnCl<sub>2</sub>, TiBr<sub>4</sub> and Y<sub>2</sub>O<sub>3</sub>. Sorption rates for all catalysts used in this study are listed in Table 2. The absorption rate is calculated between 0 and 1.3 wt. % hydrogen content, desorption rate is determined between 80 and 20% of the respective capacity. The absorption rate for HfCl<sub>4</sub> modified Na<sub>2</sub>LiAlH<sub>6</sub> is not listed due to its low capacity (1.5 wt. %).

#### 4. Conclusion

Na<sub>2</sub>LiAlH<sub>6</sub> with different catalyst additions was prepared by high-energy milling and investigated with respect to phase

formation and hydrogen absorption and desorption properties. XRD results demonstrate reversibility of the hydrogen reaction. Among the catalysts investigated in this study, TiCl<sub>3</sub> and TiF<sub>3</sub> have the strongest catalytic effects on the kinetic properties, followed by CeO<sub>2</sub>. The reduced storage capacity is attributed to the incomplete reactions, and, in case of halides, the formation of inert NaCl. The highest reversible capacity and reasonable kinetics are achieved by using CeO<sub>2</sub>.

#### References

- [1] B. Bogdanovic, M. Schwickardi, J. Alloys Compd. 253/254 (1997) 1–9.
- [2] B. Bogdanovic, R.A. Brand, A. Marjanovic, M. Schwickardi, J. Alloys Compd. 302 (2000) 36–58.
- [3] B. Bogdanovic, German Patent DE 19526434 (1995).
- [4] J. Hout, S. Boily, V. Güther, R. Schulz, J. Alloys Compd. 283 (1999) 304–306.
- [5] X.Z. Ma, T. Klassen, E. Martinez-Franco, R. Bormann, Z.Q. Mao, R. Laufs (Eds.), Clean Energies for the 21th Century, in: Proceedings of HYFORUM 2004, EFO Energie Forum GmbH, Berlin, 2004, pp. 225–233.
- [6] E. Martinez-Franco, X.Z. Ma, T. Klassen, R. Bormann, submitted for publication.
- [7] G. Sandrock, K. Gross, G. Thomas, J. Alloys Compd. 339 (2002) 299–308.
- [8] E.H. Majzoub, J.K. Gross, J. Alloys Compd. 356/357 (2003) 363–367.